Supporting Information:

Molecular dynamics analysis of binding of kinase inhibitors to WT EGFR and the T790M mutant

Jiyong Park[a], Joseph J. McDonald[b], Russell C. Petter[b] *, and K. N. Houk[a] *

[a] Department of Chemistry and Biochemistry,

University of California, Los Angeles, Los Angeles, CA 90095, USA

[b] Celgene Avilomics Research,

Bedford, MA 01730, USA

March 19, 2016

*Emails: rpetter@celgene.com, houk@chem.ucla.edu

Contents

1 Supporting Tables

Table S1: Summary of crystallographic structures of EGFR simulated in the manuscript

Compound	Gatekeeper	Other mutation	Conformational State	$\Delta RMSD$[a]	PDB code	Reference
AEE788	T790	N/A	Active	0.39	2J6M	[S1]
AEE788	T790M	N/A	Active	0.92	2JIU	[S2]
AEE788	T790	L858R	Active	0.36	2ITT	[S1]
AMPPNP	T790	N/A	Cdk/Src-like	1.34	2GS7	[S3]
AMPPNP	T790	L858R	Active	0.43	2EB3	[S4]
Gefitinib	T790	G719S	Active	0.0	2ITO	[S1]
Gefitinib	T790	L858R	Active	0.39	2ITZ	[S1]
Gefitinib	T790M	G719S	Active	0.42	3UG2	[S4]
WZ4002	T790M	N/A	Active	0.79	3IKA	[S5]

[a] Backbone root-mean-squared deviation to an active state crystal structure (2ITO) in Å.

Table S2: Summary of MD simulations performed

Section	Type	Ens.[a]	Conf. state	Mutation	Net simulation time
Sec. 2.1	Thermodyn. integ. (TI)	NPT	Active	WT, T790M, & L858R	400 – 500 ns
Sec. 2.2	Metadynamics MD	NPT	Active & Inactive	WT	2.7 μs
Sec. 2.2	Constant temp. MD	NPT	Active	WT	250 ns
Sec. 2.4	Constant temp. MD	NPT	Active	WT & T790M	250 ns
Sec. 2.4	Metadynamics MD	NPT	Active	WT	300 ns
Sec. 2.5	Constant temp. MD	NPT	Active	WT & T790M	60 ns
Sec. 2.5	Metadynamics MD	NPT	Active	WT & T790M	150 ns
Sec. 2.6	Thermodyn. integ. (TI)	NPT	Active	T790M	400 ns

[a] NPT stands for constant number of particles, pressure, and temperature.

Table S3: Selected regions of EGFR for the computation of RMSD values for metadynamics simulations in Sec. 2.2. The seleted atoms are rendered in Fig. S5.

Atom selection	Residues number
All heavy atoms	718–719, 726, 728, 743 – 745, 762, 766, 775, 777, 788, 789, 791 – 797, 800, 841 – 842, 844, 853 – 864, 759 – 768, 858
Backbone atoms	713 – 721, 724 – 733, 722 – 750, 769 – 781, 786 – 791, 798 – 804, 812 – 828, 843 – 853, 854 – 878, 893 – 908, 923 – 929, 941 – 950, 961 – 971

2 Supporting Figures

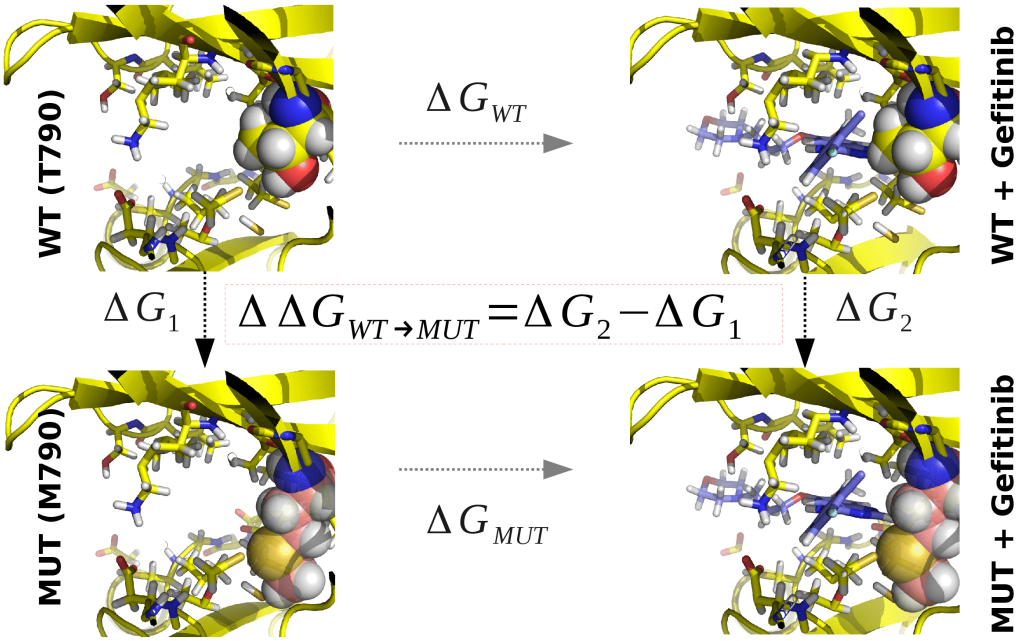

Figure S1: Overview of thermodynamic integration (TI) simulation. The equilibrium between free and bound inhibitor is determined by absolute binding free energy (ΔG). Alchemical transformations (ΔG_1 and ΔG_2) enables the computation of relative binding free energy ($\Delta\Delta G$).

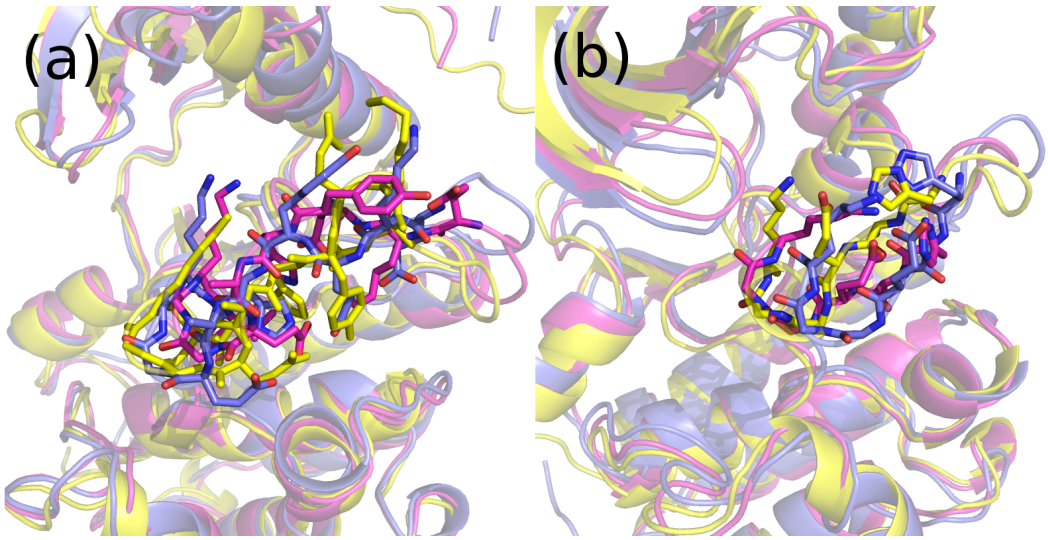

Figure S2: Overlay of the activation loop modeled using ModLoop webserver: (a) the active state of EGFR and (b) the inactive state of EGFR. The intial models built on the crystal structures are colored in yellow. Two other models (red and blue) were built upon two MD simulations at 125 ns and 250 ns, starting from the initial models.

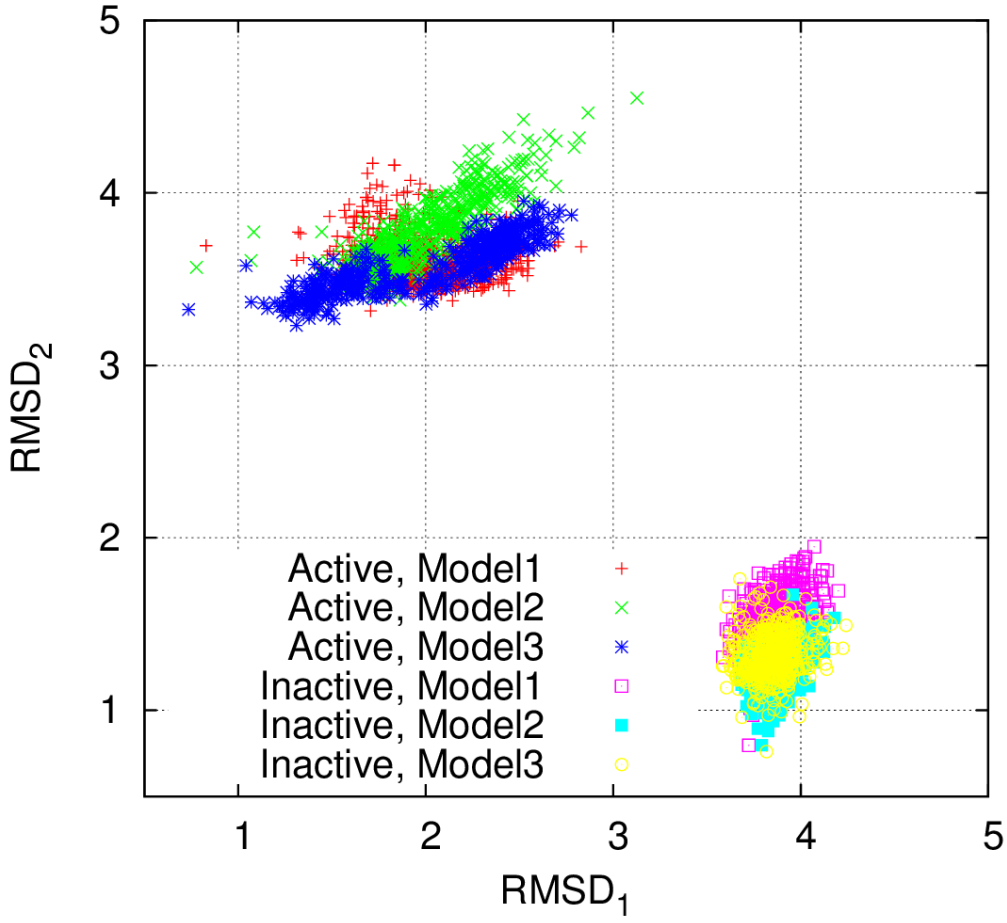

Figure S3: Conformations sampled from MD trajectories started from different activation loop conformations.

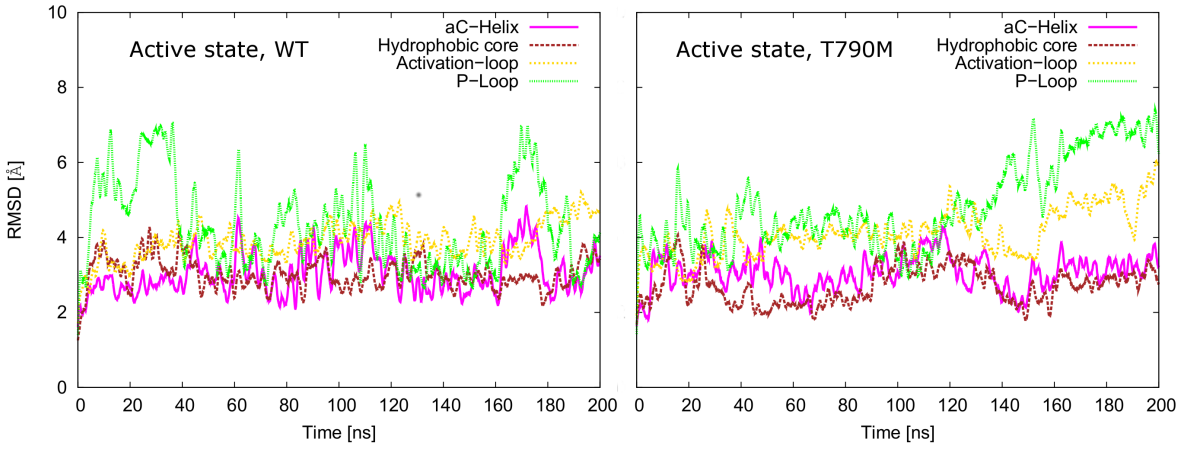

Figure S4: RMS fluctuation of the structural regions defined in Fig. 11

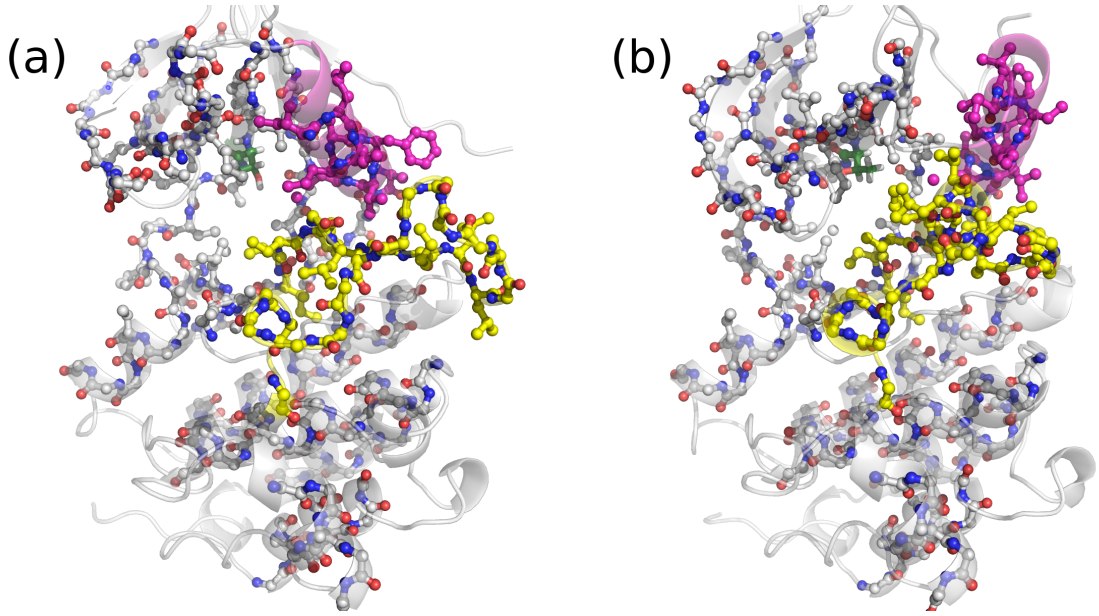

Figure S5: Atoms used to compute RMSD deviation: (a) the active state of EGFR (PDB code: 2ITO) and (b) the inactive state of EGFR (PDB code: 2GS7). Balls and sticks represent the atoms included for the RMSD calculations.

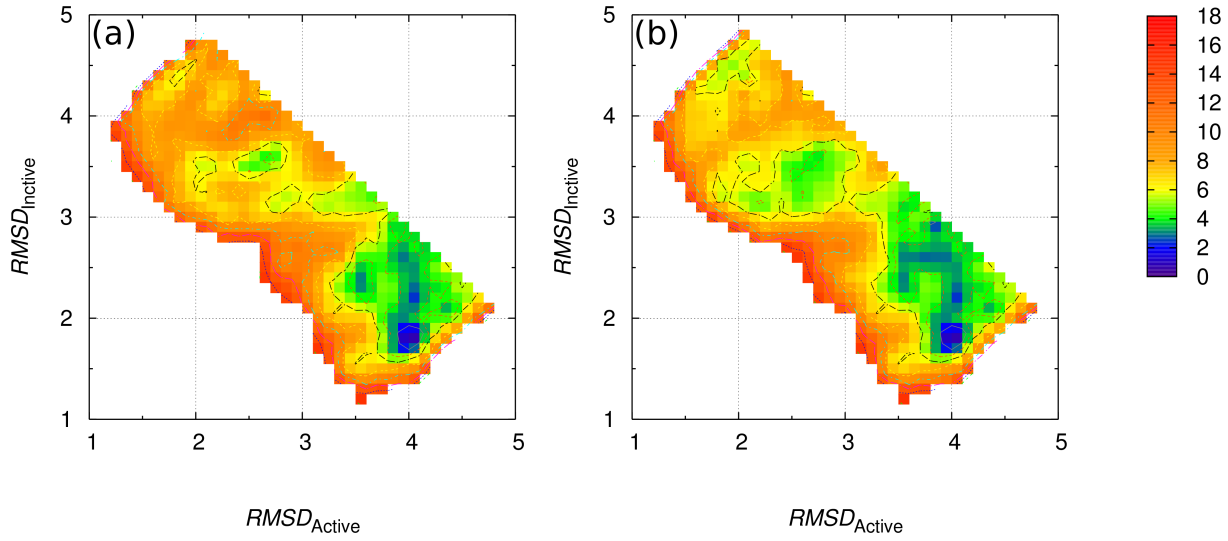

Figure S6: Convergence of the metadynamics MD simulations of the WT EGFR. The free energy profile is plotted at (a) 2.4 μs and (b) 2.7 μs.

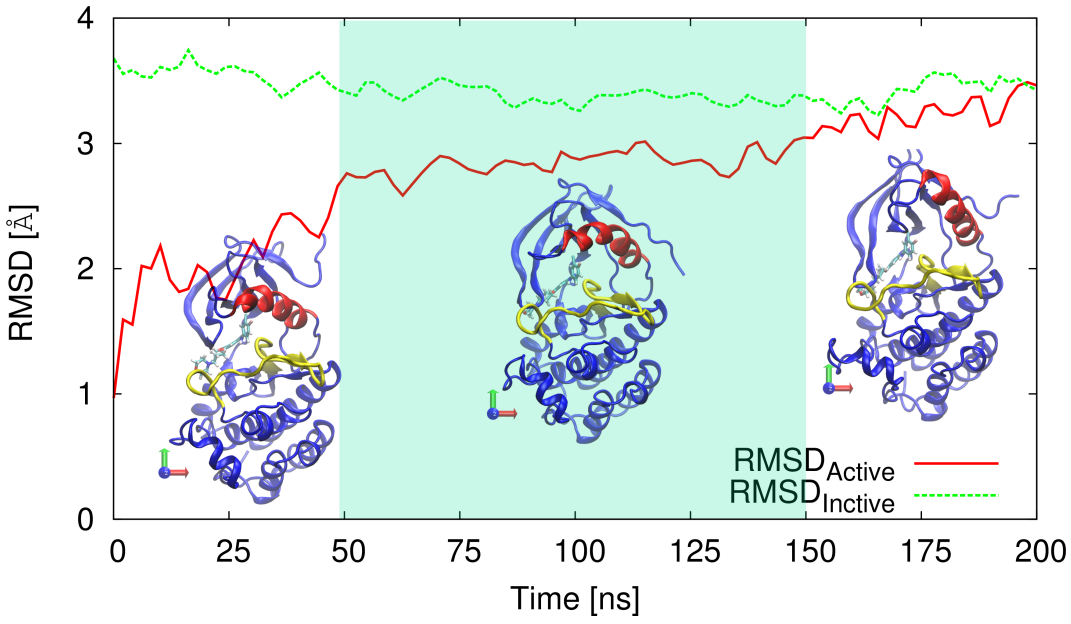

Figure S7: Constant temperature MD simulation of the T790M mutant bound to gefitinib. RMSD deviation to the active state crystal structure (PDB Code: 2ITO) and the inactive state crystal structure (PDB Code: 2GS7) are plotted. Representative conformations of 0 to 50 ns, 50 ns to 150 ns, and 150 ns to 200 ns periods are shown. The αC-helix (red) shows significant fluctuation, whereas the activation–loop (yellow) remains stable.

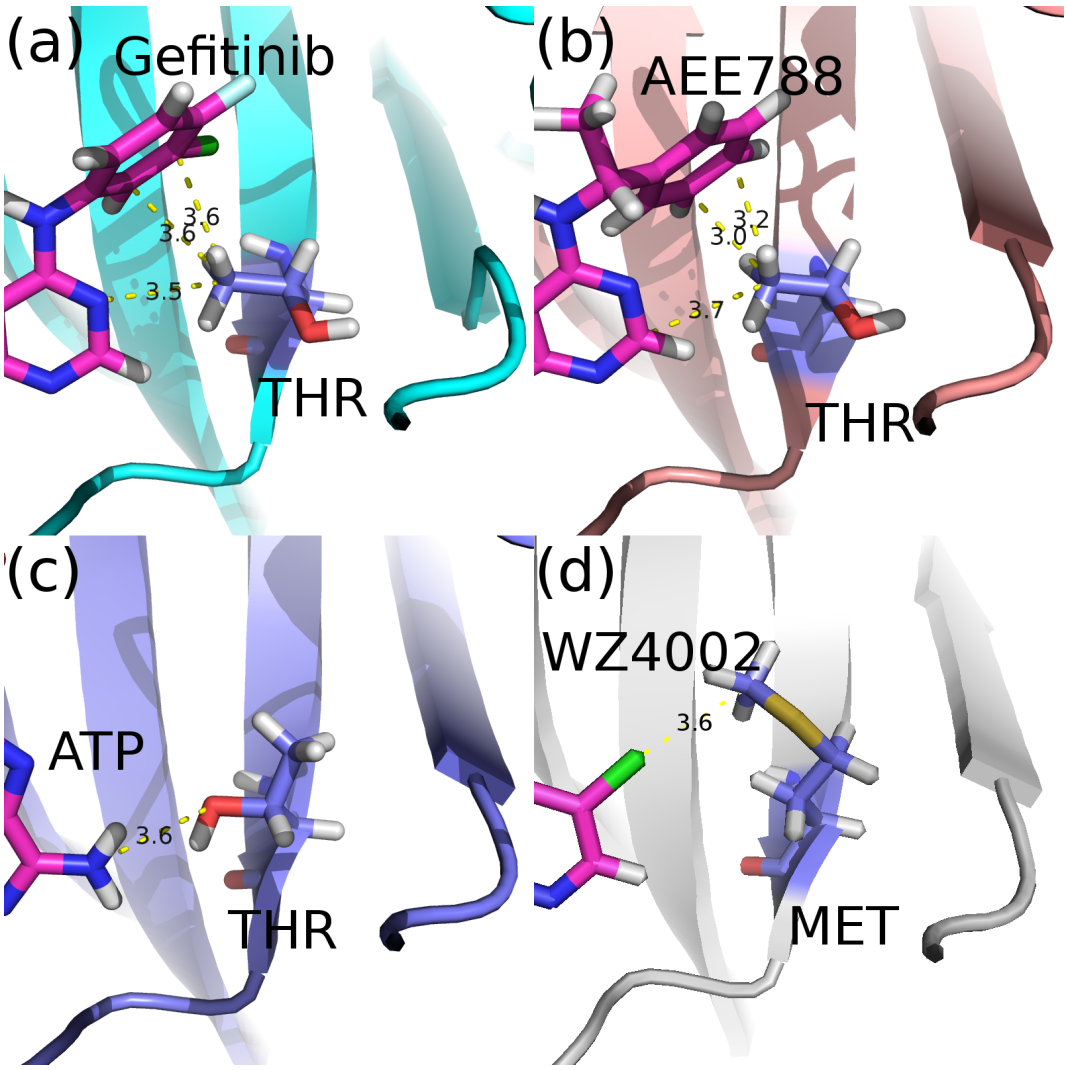

Figure S8: Interaction of gatekeeper residues and small molecules. (a) threonine gatekeeper and gefitinib (PDB Code: 2ITO), (b) threonine gatekeeper and AEE788 (PDB Code: 2J6M), (c) methionine gatekeeper with ATP (PDB Code: 3EB3), and (d) methionine gatekeeper and WZ4002 (PDB Code: 3IKA).

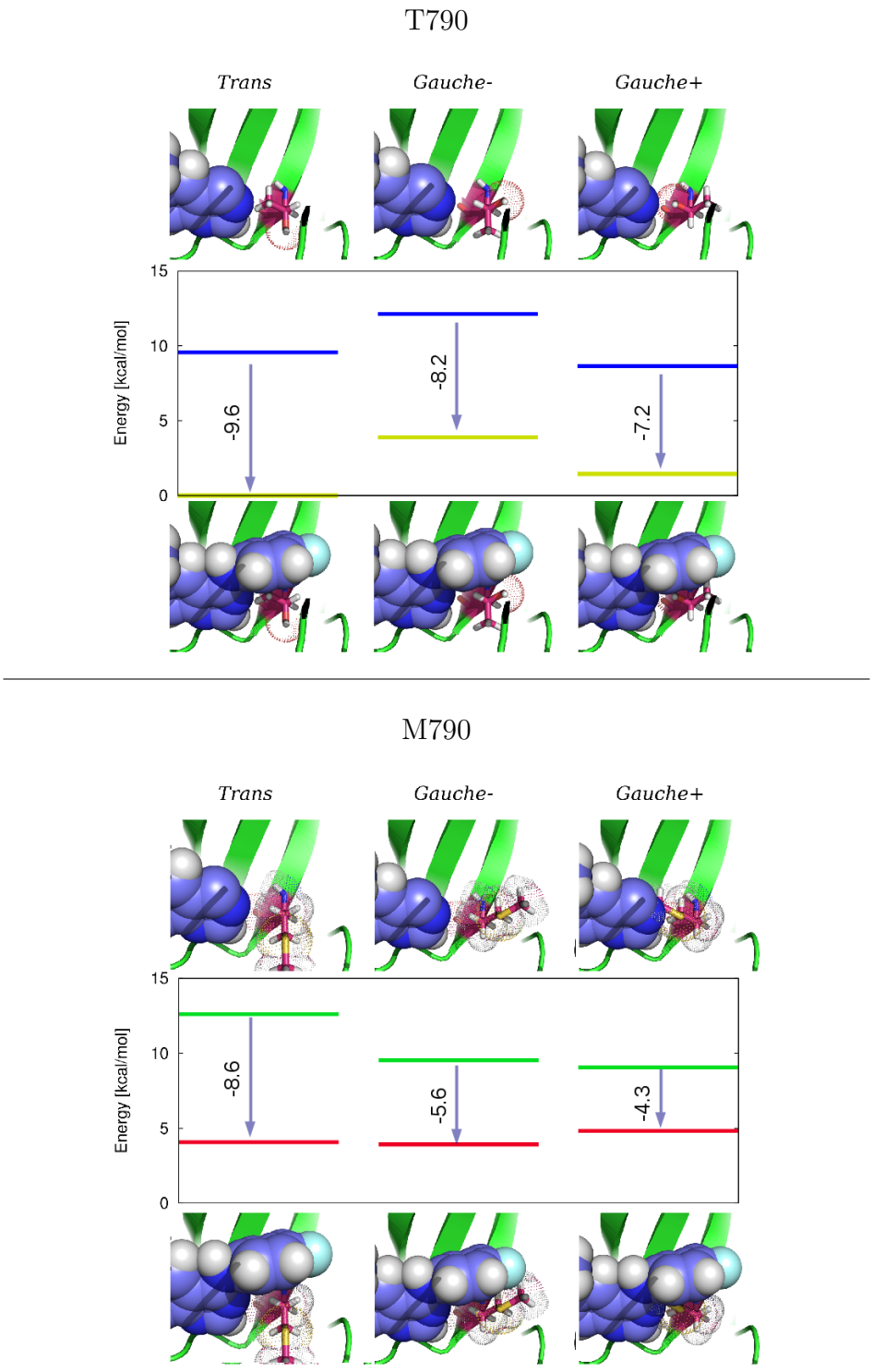

Figure S9: Binding energy contributions of the 3-chloro-4-fluoroaniline substituent of gefitinib in each conformation of the WT and T790M.

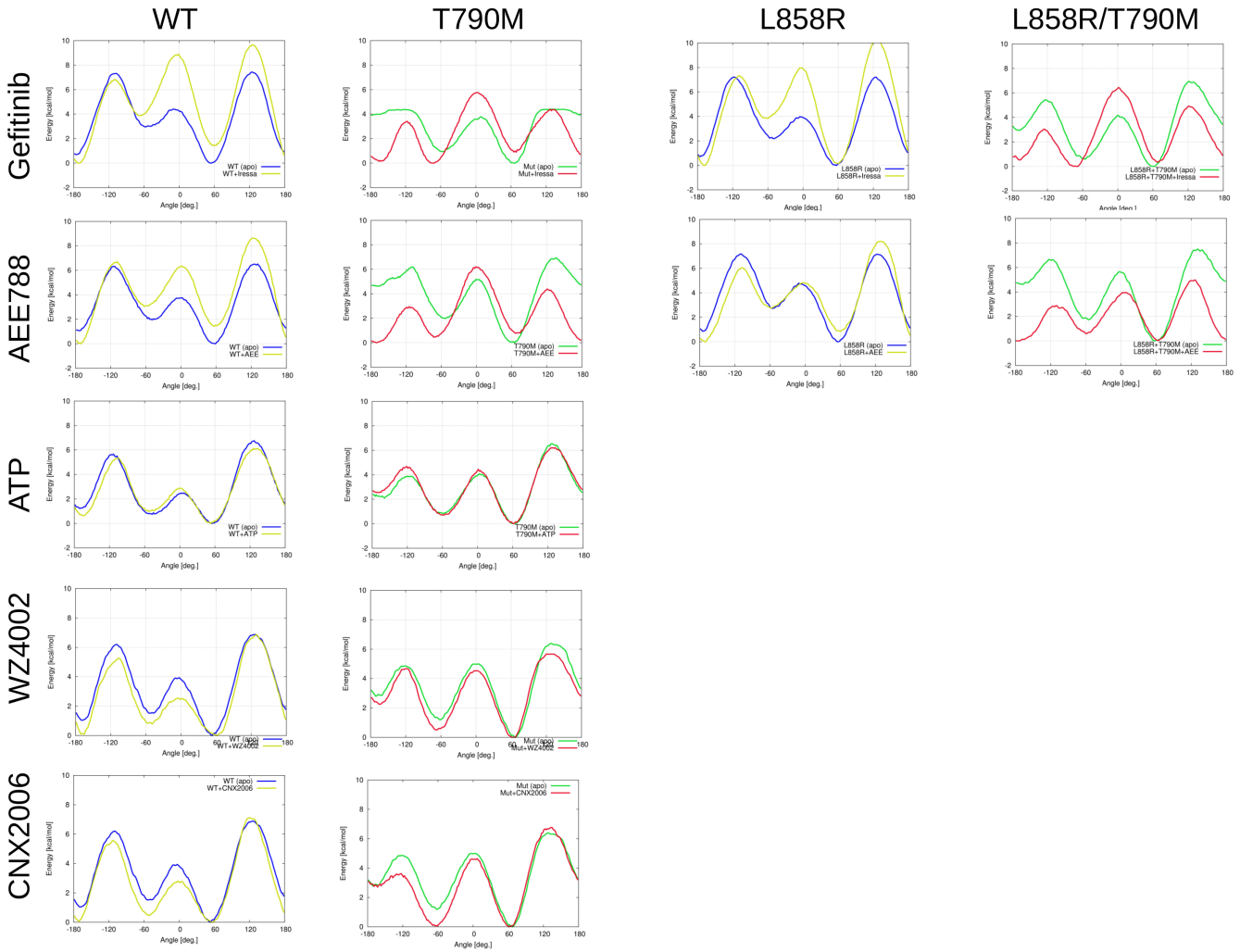

Figure S10: Free energy profiles of χ_1 dihedral angle of gatekeeper residues.

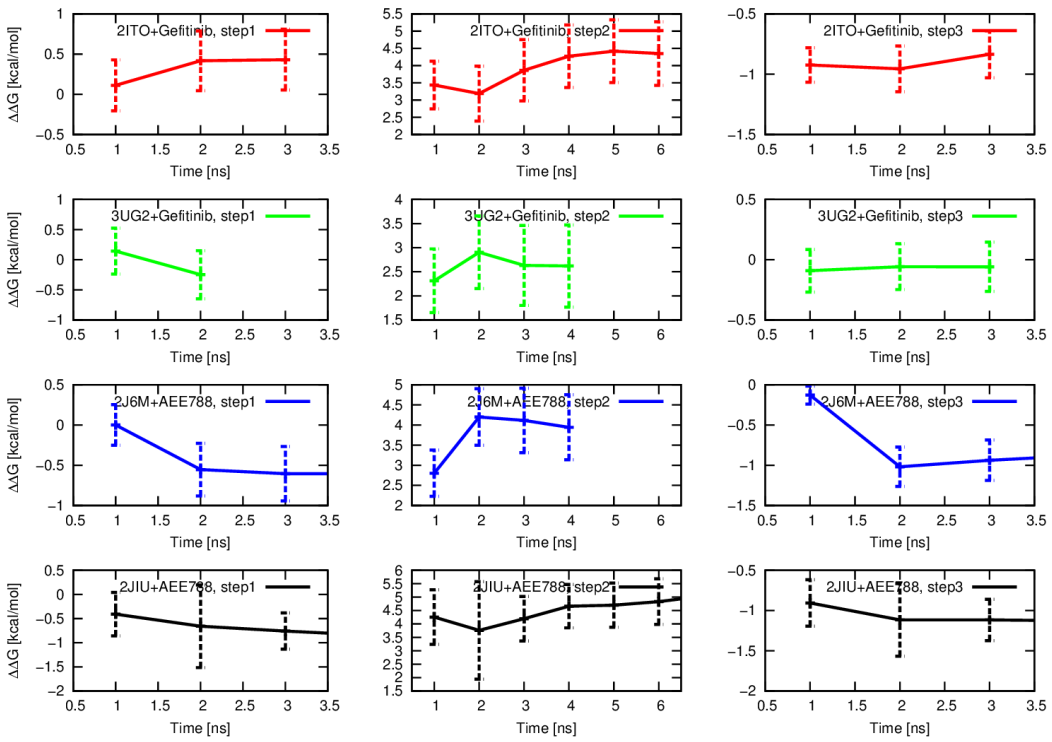

Figure S11: Statistical convergence of TI simulations

References

[S1] Yun, C.-H., Boggon, T. J., Li, Y., Woo, M. S., Greulich, H., Meyerson, M., and Eck, M. J. (2007) Structures of lung cancer-derived EGFR mutants and inhibitor complexes: mechanism of activation and insights into differential inhibitor sensitivity. *Cancer Cell 11*, 217–227.

[S2] Yun, C.-H., Mengwasser, K. E., Toms, A. V., Woo, M. S., Greulich, H., Wong, K.-K., Meyerson, M., and Eck, M. J. (2008) The T790M mutation in EGFR kinase causes drug resistance by increasing the affinity for ATP. *Proc. Natl. Acad. Sci. U. S. A. 105*, 2070–2075.

[S3] Zhang, X., Gureasko, J., Shen, K., Cole, P. A., and Kuriyan, J. (2006) An allosteric mechanism for activation of the kinase domain of epidermal growth factor receptor. *Cell 125*, 1137–1149.

[S4] Yoshikawa, S. et al. (2013) Structural basis for the altered drug sensitivities of non-small cell lung cancer-associated mutants of human epidermal growth factor receptor. *Oncogene 32*, 27–38.

[S5] Zhou, W., Ercan, D., Chen, L., Yun, C.-H., Li, D., Capelletti, M., Cortot, A. B., Chirieac, L., Iacob, R. E., Padera, R., Engen, J. R., Wong, K.-K., Eck, M. J., Gray, N. S., and Jnne, P. A. (2009) Novel mutant-selective EGFR kinase inhibitors against EGFR T790M. *Nature 462*, 1070–1074.